

Rapid and Accurate Assessment of Road Damage by Integrating Data from Mobile Camera Systems (MCS) and Mobile LiDAR Systems (MLS)

February
2024

A Research Report from the Pacific Southwest
Region University Transportation Center

Qi Chen, University of Hawai'i at Mānoa, Department of Geography &
Environment



UNIVERSITY
of HAWAII®
MĀNOA

TECHNICAL REPORT DOCUMENTATION PAGE

1. Report No. PSR-21-72		2. Government Accession No. N/A		3. Recipient's Catalog No. N/A	
4. Title and Subtitle Rapid and Accurate Assessment of Road Damage by Integrating Data from Mobile Camera Systems (MCS) and Mobile LiDAR Systems (MLS)				5. Report Date 2024/1/26	
				6. Performing Organization Code N/A	
7. Author(s) Qi Chen, 0000-0003-0110-7996				8. Performing Organization Report No. TBD	
9. Performing Organization Name and Address METRANS Transportation Center University of Southern California University Park Campus, RGL 216 Los Angeles, CA 90089-0626				10. Work Unit No. N/A	
				11. Contract or Grant No. USDOT Grant 69A3551747109	
12. Sponsoring Agency Name and Address U.S. Department of Transportation Office of the Assistant Secretary for Research and Technology 1200 New Jersey Avenue, SE, Washington, DC 20590				13. Type of Report and Period Covered Final report (2021/07/01 – 2024/1/26)	
				14. Sponsoring Agency Code USDOT OST-R	
15. Supplementary Notes METRANS Project webpage: https://metrans.org/research/rapid-and-accurate-assessment-of-road-damage-by-integrating-data-from-mobile-camera-systems-mcs-and-mobile-lidar-systems-mls-can-we-get-the-best-of-both-worlds- Report DOI: https://doi.org/10.25554/9hwx-3y87 Data: https://datadryad.org/stash/dataset/doi:10.5061/dryad.4mw6m90jc					
16. Abstract We developed a novel methodology of generating georeferenced, very detailed (at millimeter spatial resolution) orthomosaics of road surface using panoramic photos taken from mobile camera system and Structure-from-Motion technology.					
17. Key Words Mobile mapping, road condition assessment, orthomosaic			18. Distribution Statement No restrictions.		
19. Security Classif. (of this report) Unclassified		20. Security Classif. (of this page) Unclassified		21. No. of Pages 34	22. Price N/A

Form DOT F 1700.7 (8-72)

Reproduction of completed page authorized

Contents

Acknowledgements.....	5
Abstract.....	6
Executive Summary.....	7
Introduction	8
Data and Methods	12
Study Area and Data	12
Methods.....	14
Results and Discussion	17
Orthomosaics after masking ego-vehicle	20
Orthomosaics after masking ego-vehicle and sky	21
Orthomosaics after masking ego-vehicle, sky, and moving street objects	25
Visual Assessment of Road Conditions and Damage.....	28
Conclusions	31
References	32
Data Management Plan	34

About the Pacific Southwest Region University Transportation Center

The Pacific Southwest Region University Transportation Center (UTC) is the Region 9 University Transportation Center funded under the US Department of Transportation's University Transportation Centers Program. Established in 2016, the Pacific Southwest Region UTC (PSR) is led by the University of Southern California and includes seven partners: Long Beach State University; University of California, Davis; University of California, Irvine; University of California, Los Angeles; University of Hawaii; Northern Arizona University; Pima Community College.

The Pacific Southwest Region UTC conducts an integrated, multidisciplinary program of research, education and technology transfer aimed at *improving the mobility of people and goods throughout the region*. Our program is organized around four themes: 1) technology to address transportation problems and improve mobility; 2) improving mobility for vulnerable populations; 3) Improving resilience and protecting the environment; and 4) managing mobility in high growth areas.

U.S. Department of Transportation (USDOT) Disclaimer

The contents of this report reflect the views of the authors, who are responsible for the facts and the accuracy of the information presented herein. This document is disseminated in the interest of information exchange. The report is funded, partially or entirely, by a grant from the U.S. Department of Transportation's University Transportation Centers Program. However, the U.S. Government assumes no liability for the contents or use thereof.

Disclosure

Principal Investigator, Co-Principal Investigators, others, conducted this research titled, "Rapid and Accurate Assessment of Road Damage by Integrating Data from Mobile Camera Systems (MCS) and Mobile LiDAR Systems (MLS)" at the University of Hawai'i at Mānoa, Department of Geography & Environment. The research took place from 2021/07/01 to 2024/01/26 and was funded by a grant from the Pacific Southwest Region UTC in the amount of \$29,983. The research was conducted as part of the Pacific Southwest Region University Transportation Center research program.

Acknowledgements

Great thanks are extended to Mr. Eric Yamashita and the National Disaster Preparedness Training Center (NDPTC) for providing the NCTECH iStar Pulsar mobile mapping system to capture 360-degree imagery.

Abstract

In this project, we devised an innovative approach to produce highly detailed orthomosaics of road surfaces, with a spatial resolution as fine as millimeters, utilizing panoramic photos obtained from a mobile camera system combined with Structure-from-Motion technology. Our method emphasizes the necessity of accurately masking out the ego-vehicle (the vehicle carrying the camera), the sky, and any moving objects (such as cars, bicycles, and pedestrians) present in the street scenes captured by the photos. We employed a combination of deep learning, image processing techniques, and manual editing to perform this masking process. It was observed that removing these objects from the images facilitates precise photo alignment and often leads to a substantial enhancement in the quality of the orthomosaics. We tested our methodology at three different sites across two different islands with contrasting traffic conditions and surrounding environments (campus, urban, and rural). We found that the resulting orthomosaics are readily applicable for GIS analysis and the assessment of road conditions and damages. Moving forward, the methodology could be refined further by automating the masking process, particularly through the integration of deep learning models. Additionally, we discovered that the timing of photo capture significantly influences the quality of the orthomosaic, with midday proving to be a preferable time window compared to early morning or late afternoon to minimize shadow effects in the orthomosaics.

Rapid and Accurate Assessment of Road Damage by Integrating Data from Mobile Camera Systems (MCS) and Mobile LiDAR Systems (MLS)

Executive Summary

This report presents a novel methodology developed for generating highly detailed orthomosaics of road surfaces, achieving millimeter-level spatial resolution. The approach utilizes panoramic photos obtained from a mobile camera system, coupled with Structure-from-Motion (SfM) technology. A key aspect of the methodology is the accurate masking of the ego-vehicle, sky, and moving objects (such as vehicles, bicycles, and pedestrians) present in the street scenes captured by the photos. This masking process involves a combination of deep learning algorithms, image processing techniques, and manual editing. The study demonstrates that removing these objects from the images significantly improves photo alignment precision and enhances the overall quality of the orthomosaics. The resulting orthomosaics are found to be highly applicable for GIS analysis and the assessment of road conditions and damages. Additionally, the report discusses potential avenues for further refinement of the methodology, particularly through the automation of the masking process using deep learning models. Furthermore, the research reveals the importance of timing in photo capture, highlighting midday as the optimal time window to minimize shadow effects in the orthomosaics, compared to early morning or late afternoon. Overall, this innovative methodology offers promising advancements in the field of remote sensing and geospatial analysis for road infrastructure assessment.

Introduction

Natural hazards pose a significant risk to transport infrastructure and can cause an annual direct damage of 3.1 to 22 billion US dollars globally, with the 84% of it being flooding-related (Koks et al. 2019). The Hawaiian archipelago is a prime example of this due to its vulnerability to multiple hazards and threats, especially sea-level rise (SLR) and/or extreme-weather related flooding (Fletcher et al. 2010; Onat et al. 2018). For example, the 2017 Hawai'i Sea Level Rise Vulnerability and Adaptation (HSLRVA) report (HCCMAC 2017) suggested that 3.2 feet of projected SLR is possible in the state over this century. This will inundate 25,800 acres of low lying land and 38 miles of major roads. Because utilities such as water, wastewater, and electrical systems often run besides or beneath roadways, the cost for repairing vulnerable roadways, even for short distance, is enormous.

Cost-effective approaches to assess road damage and conditions are vital for repairing and reconstructing the transportation infrastructure after hazards (Jalinoos et al. 2019). Given its ability of obtaining spatially explicit information over large areas, remote sensing has become an increasingly important tool for this (Schnebele et al. 2015; Ghaffarian et al. 2018), especially with the advent of new technologies such as airborne LiDAR (Seydi & Rastiveis 2019) and unmanned aerial vehicle (UAV, Jalinoos et al. 2019). However, several factors have constrained a wider use of airborne and satellite sensors for remote sensing of roadways. First of all, most sensors, except UAV-based, have limited spatial resolutions (at best in tens of centimeters, instead of in centimeters) to detect fine-scale road damage such as cracks. Second, they might have the difficulty of frequency data acquisition (e.g., satellite imagery restricted by orbiting cycles and clouds, UAV flights restricted over urban areas). Third, the cost of data acquisition could be high, especially for aerial photography or LiDAR mapping with manned aircrafts. Finally yet importantly, objects near roadways (e.g., trees, buildings, steep terrain) often block the views of airborne and satellite sensors to road surface, resulting in incomplete data coverage.

Vehicle-based mobile mapping systems (MMSs) have enormous potentials to overcome the above challenges. A MMS typically consists of a vehicle mounted with cameras and/or laser sensors, GNSS (Global Navigation Satellite System) receivers, and an inertial measurement unit (IMU) (Wang et al. 2019). The advantages of MMS come from the fact that it can capture 2D images and/or 3D point clouds of road surface at mm- to cm-level resolutions given its proximity to road surface. Note that a wide range of MMS configurations exist, depending on the types of sensors used (laser sensors, cameras, or

both). Hereinafter, we refer to the system with only laser scanners as mobile laser system (MLS) and the one with only cameras as mobile camera system (MCS). Moreover, we use MMS for systems that integrate both sensors or as a generic term for either MLS or MCS. Typically, a MCS is several magnitudes cheaper than a MLS or a MMS equipped with both lasers and cameras.

Many transportation agencies in the United States are early adopters of MLS technologies for roadway design, construction, maintenance, and management (Olsen 2013). For example, Hawaii Department of Transportation (HDOT) has collected mobile LiDAR data of all state roads as early as in 2009 and has been repeating the acquisitions since then. Oregon DOT (ODOT) has been using survey-grade MMS to collect LiDAR point clouds since 2015 to create 3D representations of more than 12,880 km of roadways and replace traditional surveying when possible. Martin et al. (2020) found that the use of MLS in ODOT for roadway design and construction could result in \$2 saving for every \$1 invested on the technology.

Despite of its substantial benefits, the purchase and operation of MLS is a large sum. For example, the initial cost of ODOT MLS is about \$840,000 with the laser scanner alone costing ~\$750,000; in addition, a cost of ~\$100,000 per year exist for system calibration, software maintenance, and technical support, excluding the cost of collecting LiDAR data itself (Martin et al. 2020). Because of the high up-front cost, many agencies such as HDOT do not own MLS systems by themselves. Instead, they contracted the LiDAR data collection, processing, information extraction, database development to commercial companies. After a company finishes LiDAR data collection for a place in a given year, the MLS and vehicle will move to another place (which means another island or the Mainland for Hawaii) and will not return until the next year. Because of the prohibitive cost and logistic difficulty of collecting mobile LiDAR data as rapidly as needed, few studies (see, e.g., Gong & Maher 2014) have used mobile LiDAR data to assess the post-hazard road damages.

In recent years, MCS has emerged as a low-cost alternative of MLS for mobile mapping, thanks to the advances in technologies such as Structure from Motion (SfM) and Simultaneous Localization and Mapping (SLAM) (Ji et al. 2020). Modern panorama cameras cost only a few hundred to a few thousand dollars, which are very inexpensive compared to laser scanners. In addition, panorama camera imaging is essentially passive remote sensing that collect images, unlike active LiDAR remote sensing that generates massive point

clouds. This means that it does not need power generators, complex wiring and hardware design, and high-performance computers to operate the system (Fig. 1).

The main challenge with MCS, however, is that cameras themselves do not directly collect 3D information as MLS does. Instead, we need to use photogrammetry-based multi-view geometry to model the 3D coordinates of objects from a sequence of overlapping images taken from different exposure stations of the moving camera (Hartley and Zisserman 2003). In addition, a MCS, if it is built at a low cost, it is usually equipped with a low-accuracy GNSS receivers. As a result, the 3D models reconstructed from a low-cost MCS could have lower positional accuracy than the 3D models from a regular MLS. To remedy this, our original proposal is to use the precise measurements from a MLS over stable objects (such as buildings and road segments that have not been damaged by hazards) as a reference to register the 3D models derived from MCS so that we can repeatedly use MCS as a low-budget platform to monitor natural hazards while maintaining as high positional accuracy as a MLS. We expect the fusion of MCS and MLS will be able to achieve two main competing objectives in current practice: 1) produce timely, detailed, and accurate information about road damage and conditions with high spatial and temporal resolutions, and 2) lower the overall cost of operation.

However, since we started the project to collect data, we realized that the MCS system available for our project, a NCTECH iSTAR Pulsar MMS, has a GNSS receiver with a higher accuracy than we expected. We found that the positional errors of the geospatial products (e.g., orthomosaics and DEM) derived from the MCS are mostly translational, instead of additionally having scaling or rotational errors (see Fig. 1). These translational errors are as small as 1-2 meters and can be easily fixed. Therefore, we dropped the idea of using laser measurements from a MLS to register the 3D models from our MCS. This simplified our workflow. Nevertheless, there are a few new challenges that complicated our analysis when we tested the MCS in roads with busy traffic and under different environments.



Fig. 1. Orthomosaics of roadway (b) derived from our MCS data. (a) is the ArcGIS base imagery.

One important assumption of using structure-from-motion for 3D constructions from MCS photos in our project is that the objects captured in the photos should be static instead of moving. Based on this assumption, the key points from separate photos are detected, the points corresponding to the same location are matched, and then mathematical models of objects in three dimensions are derived. However, this assumption can easily be violated in the street because of the existence of moving objects such as driving cars, bikes, and pedestrians. In addition, the vehicle that mounts the camera is always captured in the image and it is moving while taking the photos (see Fig. 2). During our analysis, we also found that the sky in the photos is another area where mismatches of key points often occurs. All of these can cause confusion and erroneous results in the 3D construction process. Therefore, the main objective of this project has been revised to develop a methodology to reconstruct road surface from MCS data by minimizing the impacts of these factors.



Fig. 2. Panorama pictures that show the moving platform (car) is part of the photos.

Data and Methods

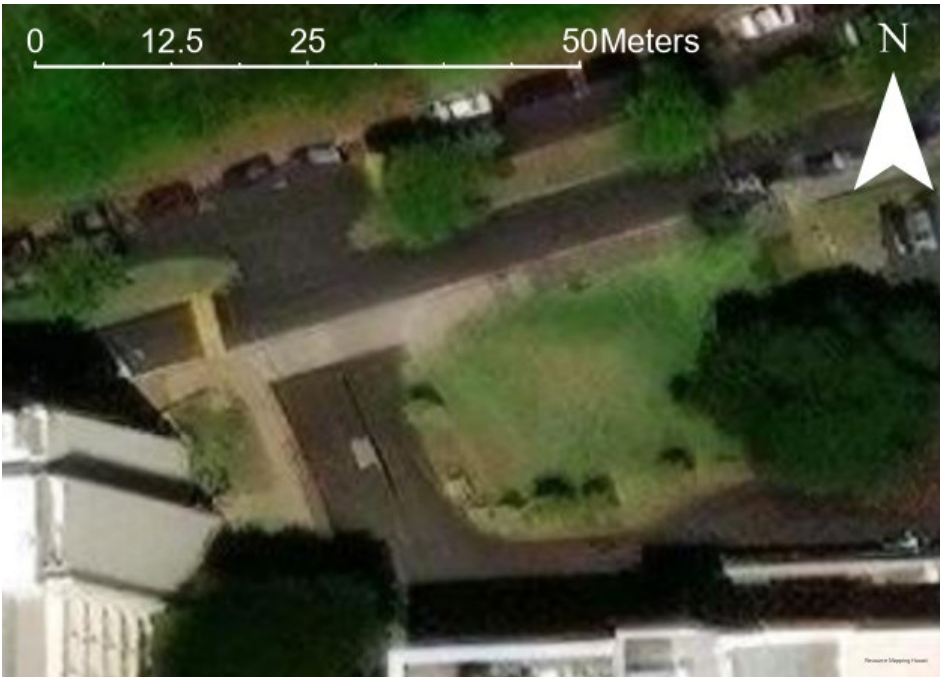
Study Area and Data

Our panoramic photos were collected using the NCTECH iSTAR Pulsar camera mounted on the roof of the vehicle (Fig. 3). This camera has a field of view of 360 x 145 degrees. The 360° degree camera is made of four cameras. Each camera can record 12.3 Megapixels (MP) and has a fisheye lens with a fixed focus and a focal length of 2.6 mm. Each of the panoramic photos has a size of 11000x5500 pixels. The system is built with a U-BLOX Neo M8N GNSS receiver with ~2.5 m accuracy and a 6-axis magnetometer IMU.



Fig. 3. The MCS system that shows the 360° degree camera mounted on top of a vehicle.

Our study areas include road segments from three different locations: 1) University of Hawaii at Manoa campus in Honolulu, hereinafter called UH, 2) Ala Manoa Boulevard in Honolulu, hereinafter called Ala Manoa, and 3) Kuhio Highway, hereinafter called Kuhio. The first two locations are in the Oahu island while the last one is in the Kauai island. The UH data were collected on June 18, 2021, when there was a pandemic lockdown on campus so there was no traffic. The Ala Manoa dataset were collected on November 21, 2022 while the Kuhio dataset were collected on December 18, 2019. Ala Manoa is in the urban Honolulu area and there are three lanes in each way while Kuhio is in the rural area of Kauai and there is only one lane in each way. There was traffic in both Ala Manoa and Kuhio. A total of 102, 272, and 100 panoramic photos were used in Kuhio, Ala Manoa, and UH, respectively, for our data analysis.



UH



Ala Manoa



Fig. 4. The three study sites: Top: UH, Middle: Ala Manoa, Bottom: Kuhio.

Methods

We reconstructed the road surface from panoramic photos using Structure from Motion (SfM) technology. Namely, SfM was used to create a 3D model and georeferenced orthoimagery of the road surface (i.e., structure) from the photos taken from the panoramic camera on the moving vehicle (i.e., motion) based on photogrammetry techniques. SfM typically involves a few important steps: 1) detection of key points, which are characteristic points on the image (e.g., corner, edge) that are usually associated with unique locations, 2) matching of key points from different photos (i.e., tie points), 3) determine the exterior and interior orientation of camera based on the tie points and GNSS measurements, 4) reconstruct the digital elevation model (DEM) of the objects captured in the photos, and 5) orthorectify the individual photos based on the DEM and exterior and interior orientation of cameras and mosaic the individual orthophotos into a orthomosaic. We used the Agisoft Metashape Professional Edition 1.8.3 for our SfM analysis. The first three steps are also called photo alignment in this software.

As mentioned in the introduction, the challenges of using SfM arise from the existence of moving objects captured in the scene, including the vehicle that carry the camera (hereinafter called ego-vehicle), driving cars, bikes, and peoples. The sky also causes a problem in generating false tie points. Masking these objects from the photo alignment process can lead to the generation of DEM and orthomosaic with a much higher quality. Therefore, our methodology

development has focused on the masking of three types of objects: 1) ego-vehicle, 2) sky, and 3) driving cars, bikes, and people, which are described as below.

Masking the ego-vehicle

In the panoramic photos, the ego-vehicle usually lies at the bottom. However, the ego-vehicle is not at the exact same location in every photo so there is no simple solution to mask the ego-vehicle (Fig. 5).



Fig. 5. Variations of ego-vehicles in the panoramic photos.

To address this issue, we developed a semi-automatic approach to mask the vehicle. First, we used the Magic Wand tool in Agisoft to click one or a few points on the vehicle in every photo, which will automatically generate initial masks for the ego-vehicle for those photos. Although these initial masks cover the majority of the vehicle, they often miss some small areas (see Fig. 6b). To address this issue, we used image processing techniques based on mathematical morphology to fill in the holes and then conduct a dilation of the mask with 100 pixels to accommodate the small variations of the ego-vehicle locations in different photos (Fig. 6c).

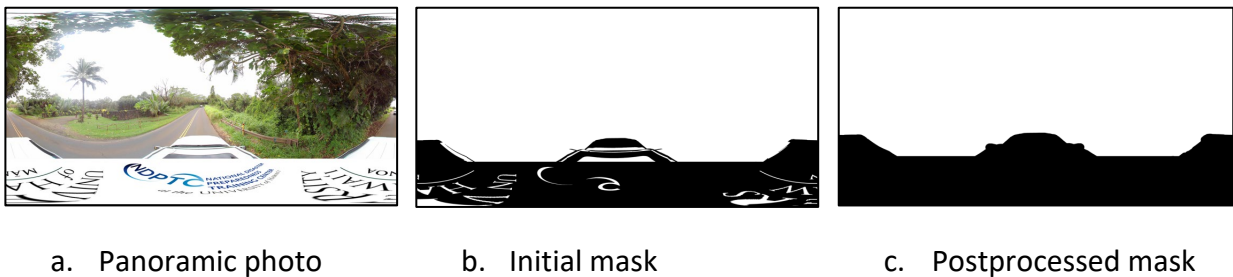


Fig. 6. Masks of ego-vehicles generated from panoramic photos.

Masking the sky

We developed a deep-learning based approach to mask the sky in every photo. This approach used a pre-trained convolutional neural network (CNN) model called Deeplab v3+ (Chen et al. 2018) that can perform semantic segmentation of the photos into different classes such as sky, building, road, car, pedestrian, and bicyclist. For the segmentation of sky, we found that there are relatively a relatively large amount of false positives in the image. To make sure we will not mask useful areas in the image for photo alignment, we only kept the largest “sky” segment (Fig. 7).

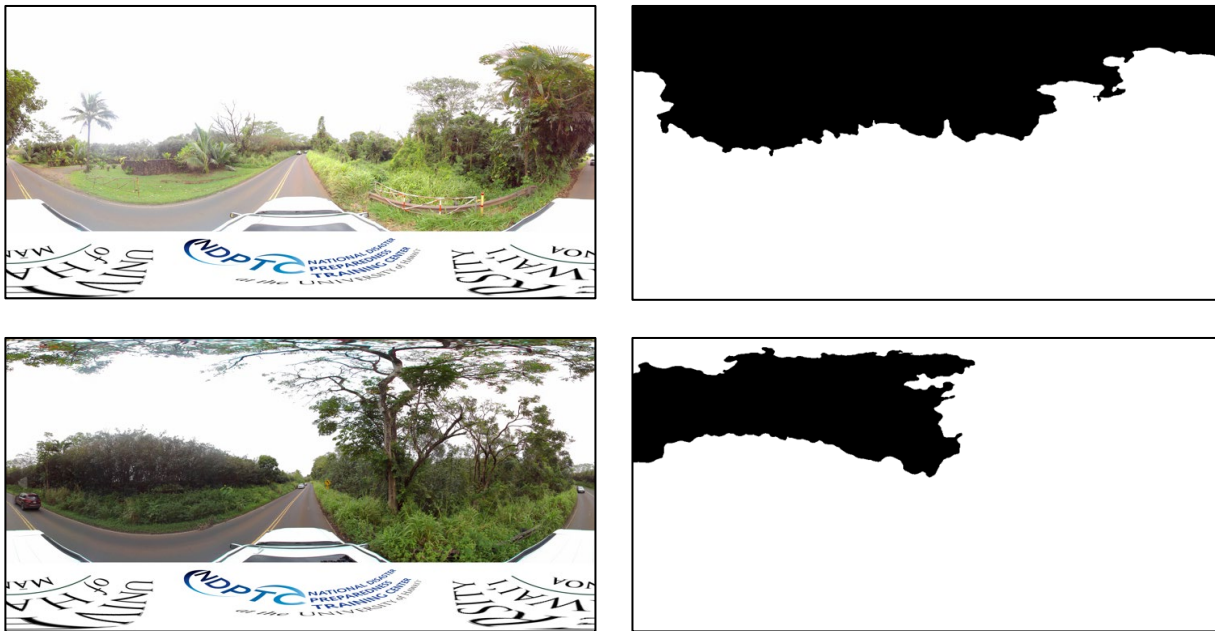


Fig. 7. Masks of sky generated from panoramic photos.

Masking driving cars, bikes, and people

We also tested the Deeplab v3+ model to segment cars, bikes, and people on the photos. However, we found that the model tended to miss small cars and it also had a relatively large amount of false positives. Therefore, we decided to manually mask these objects on the photos in the Ala Manoa and Kuhio datasets. We did not need to mask these objects for the UH dataset

because the photos were collected during the pandemic lockdown period and there were no moving cars or people in our study area during that time.

The overall workflow

Taken altogether, the overall workflow of our methodology is shown in Fig. 8. The outputted orthomosaics are already georeferenced due to the high quality photo alignment in the process so that any GIS products resulting from the road damage assessment on the orthomosaic have the associated geographic or map coordinates.

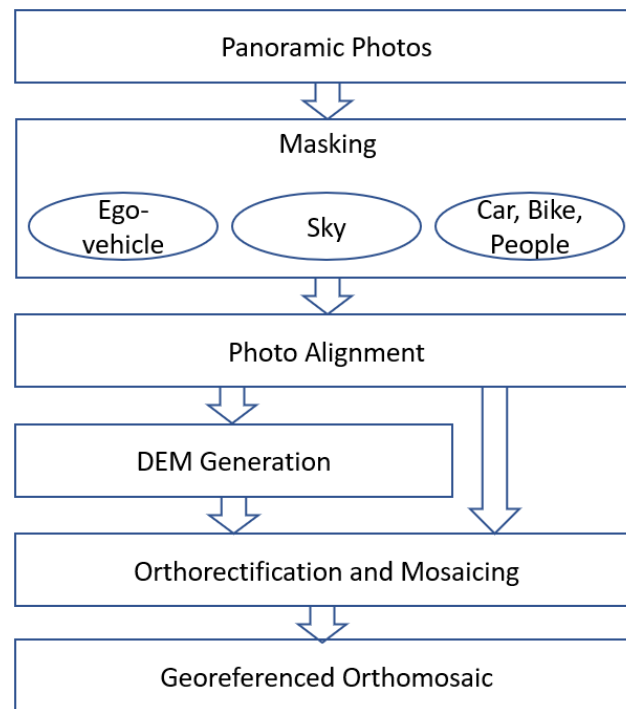


Fig. 8. Workflow of generating roadway orthomosaics from MCS photos.

Results and Discussion

We did three experiments to evaluate the impacts of masking of different objects on the quality of orthomosaics: 1) mask ego-vehicle only, 2) mask ego-vehicle and sky, and 3) mask ego-vehicle, sky, and other moving objects (car, bike, and pedestrian) on the street (Figs. 9-10).

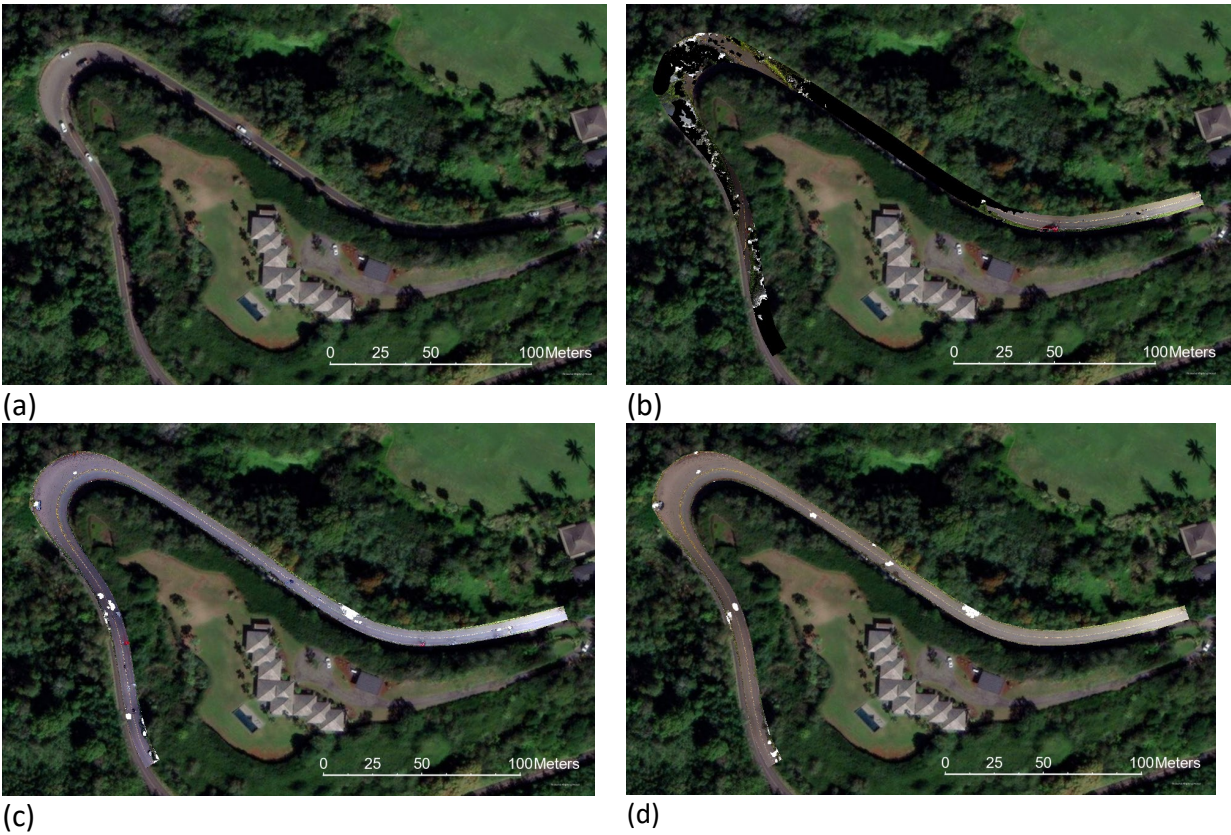
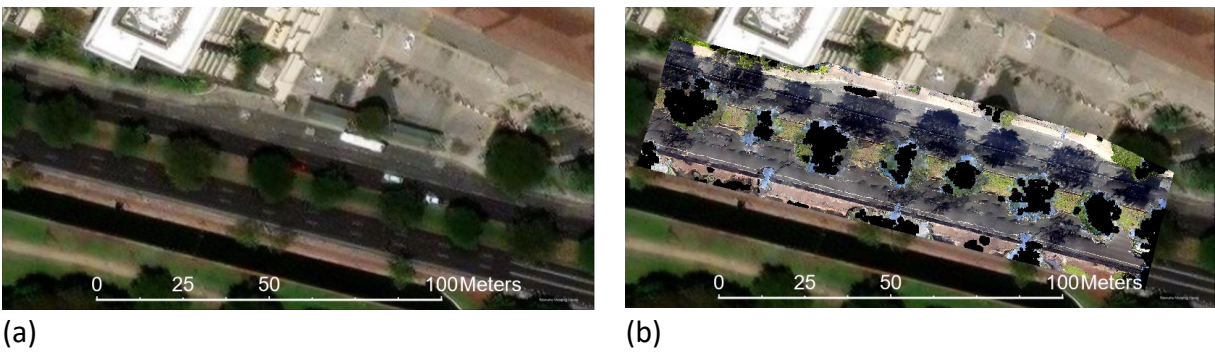


Fig. 9. Orthomosaics of Kuhio highway. (a) base imagery, (b), (c), and (d) are orthomosaics by masking the ego-vehicle, ego-vehicle + sky, and ego-vehicle + sky + street moving objects, respectively.



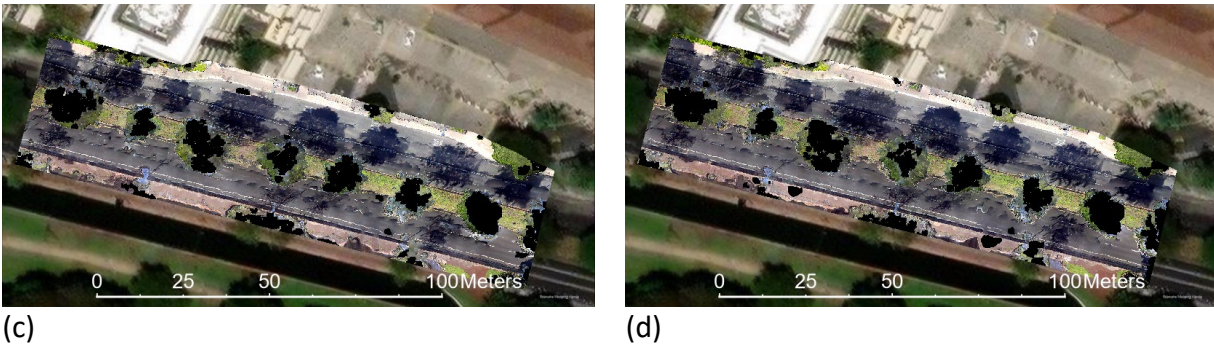


Fig. 10. Orthomosaics of Ala Manoa boulevard. (a) base imagery, (b), (c), and (d) are orthomosaics by masking the ego-vehicle, ego-vehicle + sky, and ego-vehicle + sky + street moving objects, respectively.

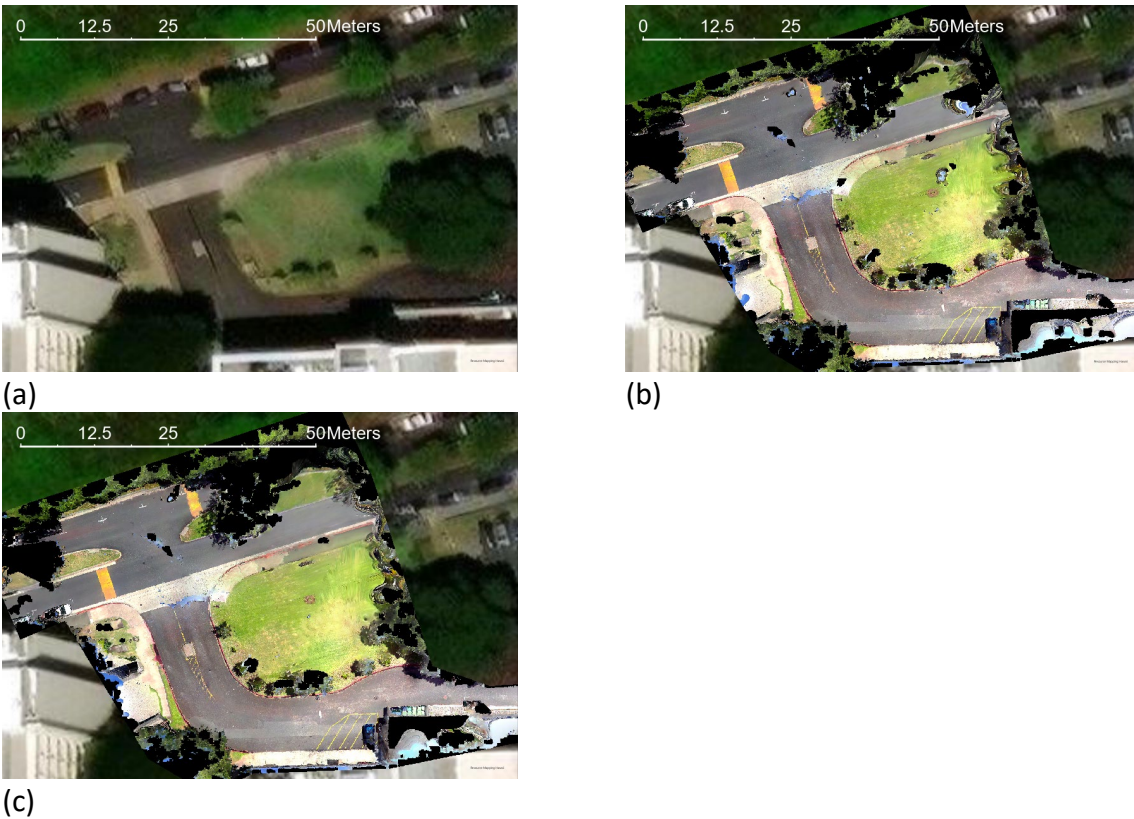


Fig. 11. Orthomosaics of UH campus road. (a) base imagery, (b) and (c) are orthomosaics by masking the ego-vehicle and ego-vehicle + sky, respectively.

Orthomosaics after masking ego-vehicle

After masking the ego-vehicle only, relatively complete orthomosaics can be generated at both UH (Fig. 11b) and Ala Manoa (Fig. 10b). We found that the Ala Manoa orthomosaic has shadows of the ego-vehicle (Fig. 12) while the UH one does not have such problems (Fig. 13). This is because the UH photos were taken at near noon time so the shadows of the vehicle are very small. The Ala Manoa photos were taken during an early morning in the weekend to minimize the traffic on the street. During the time period, the ego-vehicle casted a large shadow on the road surface, which deteriorated the quality of the orthomosaic. The large shadows casted by the trees also severely affect the quality of the orthomosaic.

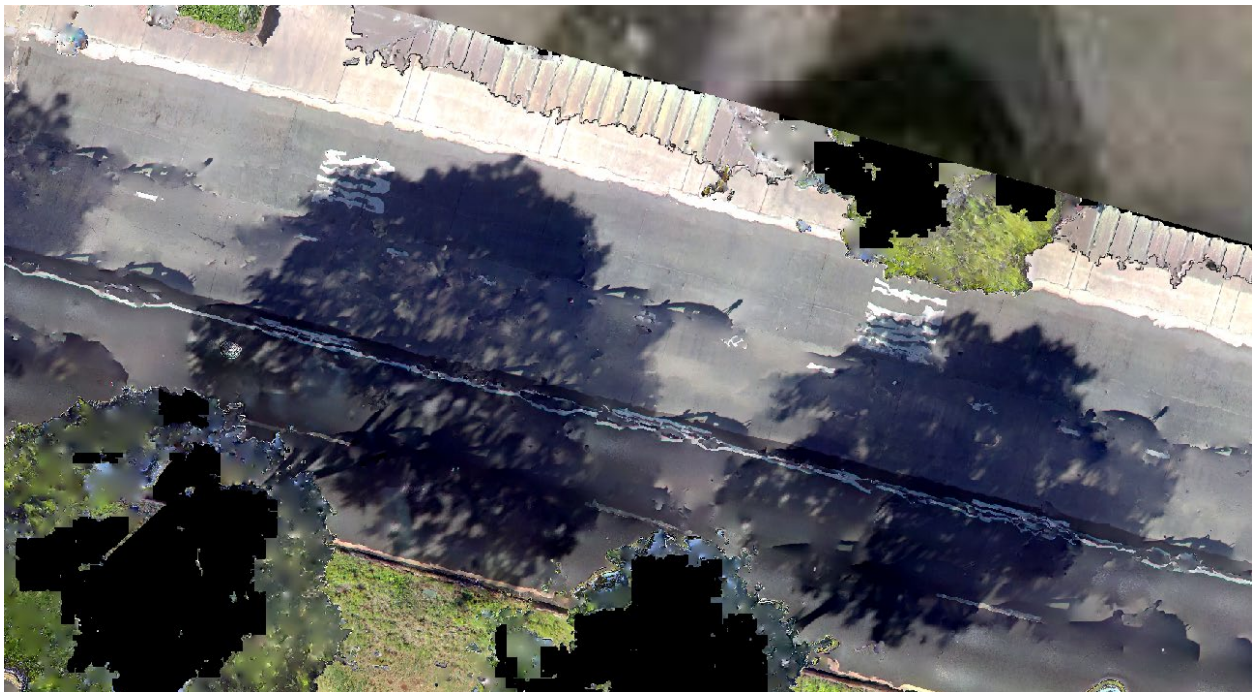


Fig. 12. Orthomosaic of Ala Manoa showing artifacts from shadows of ego-vehicles.



Fig. 13. Orthomosaic of UH showing no artifacts from shadows of ego-vehicles.

For Kuhio, a large portion of the highway failed to generate the orthomosaic (Figure Xb), which indicated that there could be photo alignment errors caused by sky or moving cars.

Orthomosaics after masking ego-vehicle and sky

For UH, we found that masking the sky in the photo has made negligible difference in the quality of orthomosaic. Here, the driving way is near a tall building so the view of sky in each photo is relatively small. A lot of characteristic key points can be generated from the building for photo alignment. This can explain why masking the sky made little difference in the orthomosaics (Figs 11b, 11c).

For Ala Manoa, we also found that masking the sky in the photo has made only small difference in the quality of orthomosaic (Fig. 14). This can be attributed to the same reason of having relatively tall buildings near the street for photo alignment.

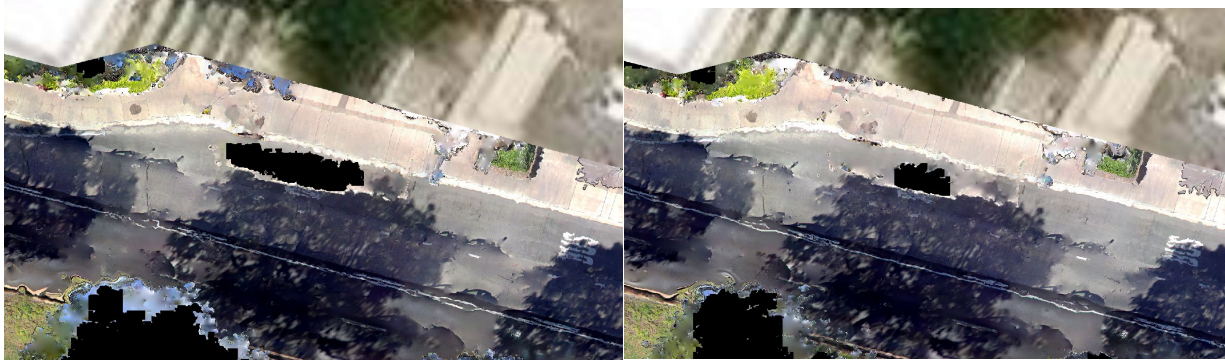


Fig. 14. Masking the sky (left: before, right: after) at Ala Manoa shows small impacts on orthomosaic quality.

However, we found that the masking of sky fixed most of the photo alignment errors at Kuhio (Figs. 15-17).



(a)



(b)

Fig. 15. Masking the sky at Kuhio shows substantial improvements on orthomosaic (a: before, b: after) quality.



(a)



(b)

Fig. 16. Masking the sky at Kuhio shows substantial improvements on orthomosaic (a: before, b: after) quality.

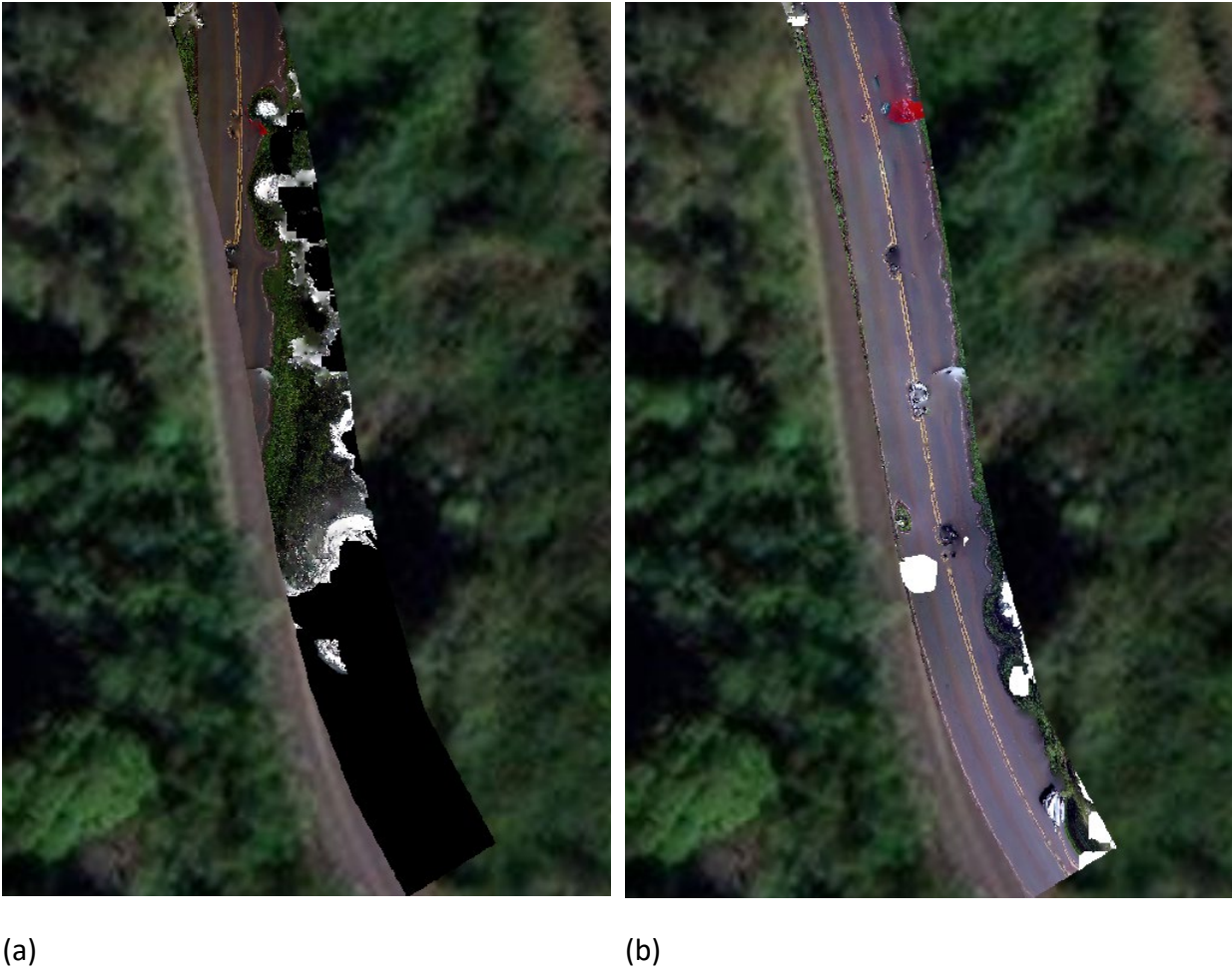


Fig. 17. Masking the sky at Kuhio shows substantial improvements on orthomosaic (a: before, b: after) quality.

Orthomosaics after masking ego-vehicle, sky, and moving street objects

For Kuhio, we noticed that artifacts corresponding to driving cars still exist in the orthomosaics after masking the ego-vehicle and sky. Most of these artifacts were removed after masking the driving cars (Figs 18-19).

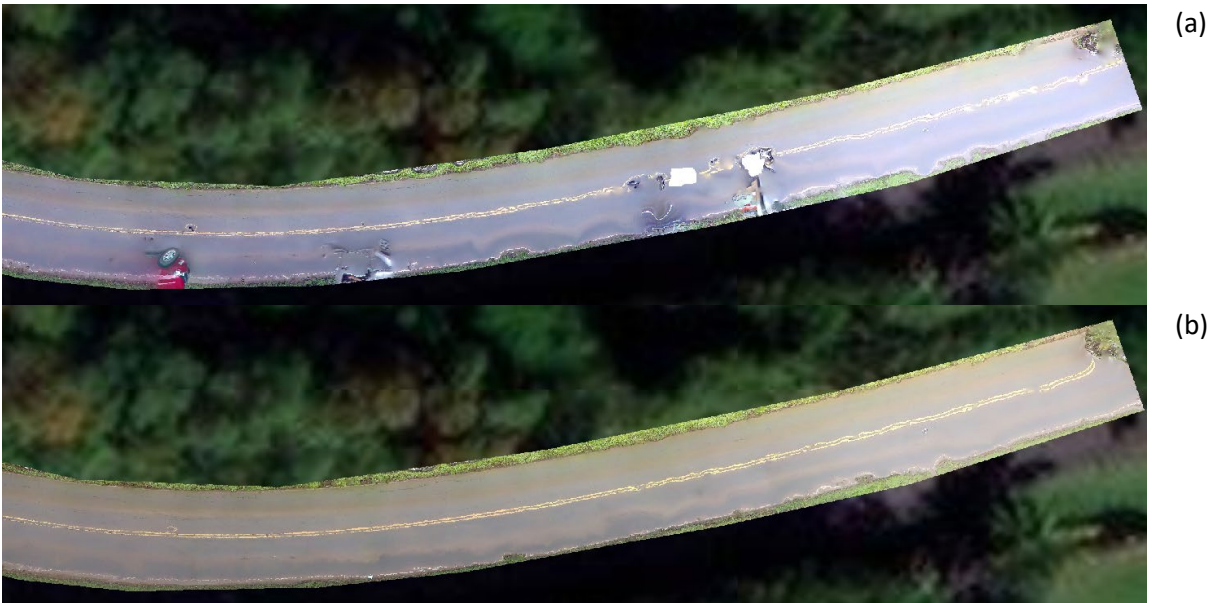


Fig. 18. Masking the cars on the roadway at Kuhio shows substantial improvements on orthomosaic (a: before, b: after) quality.

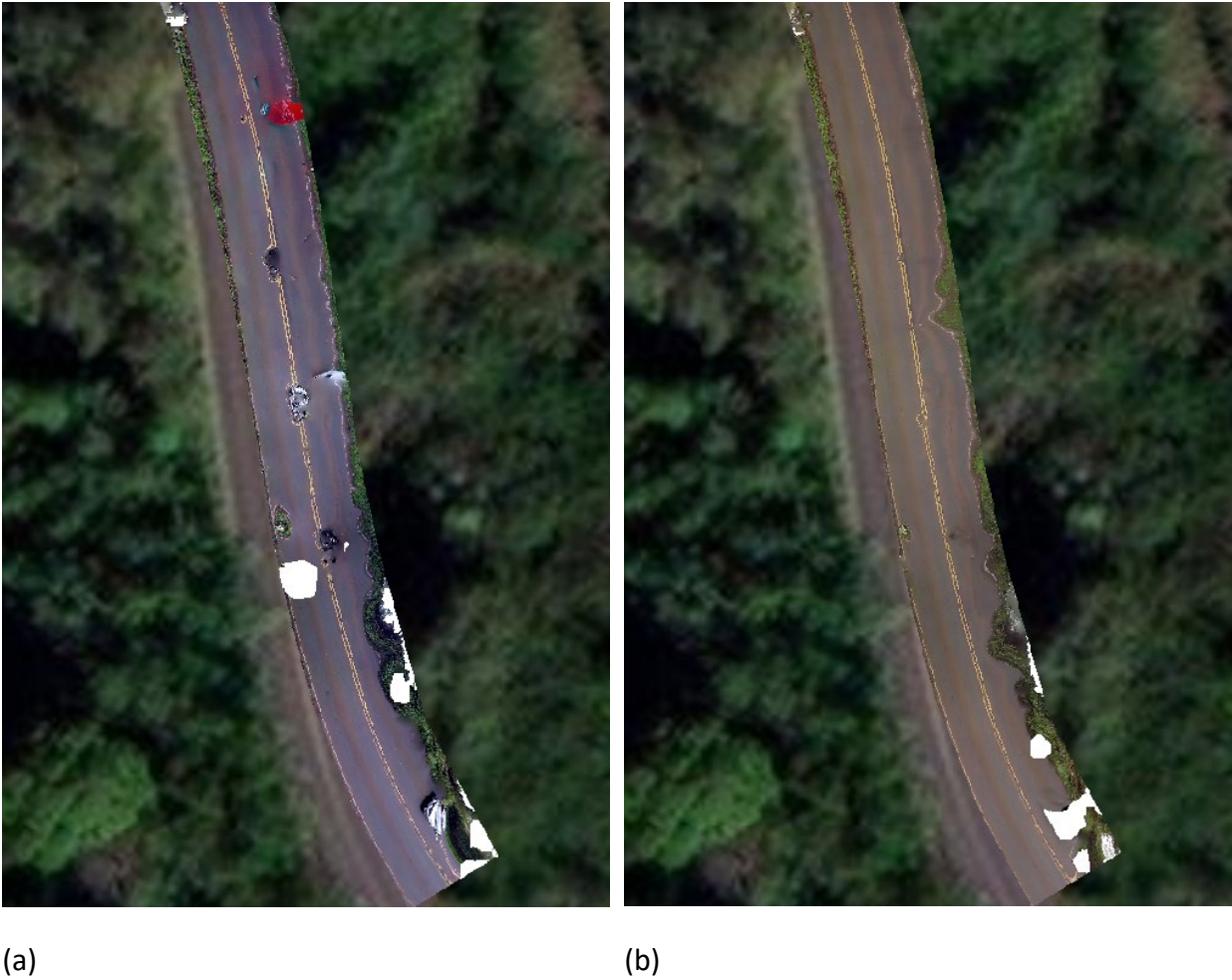
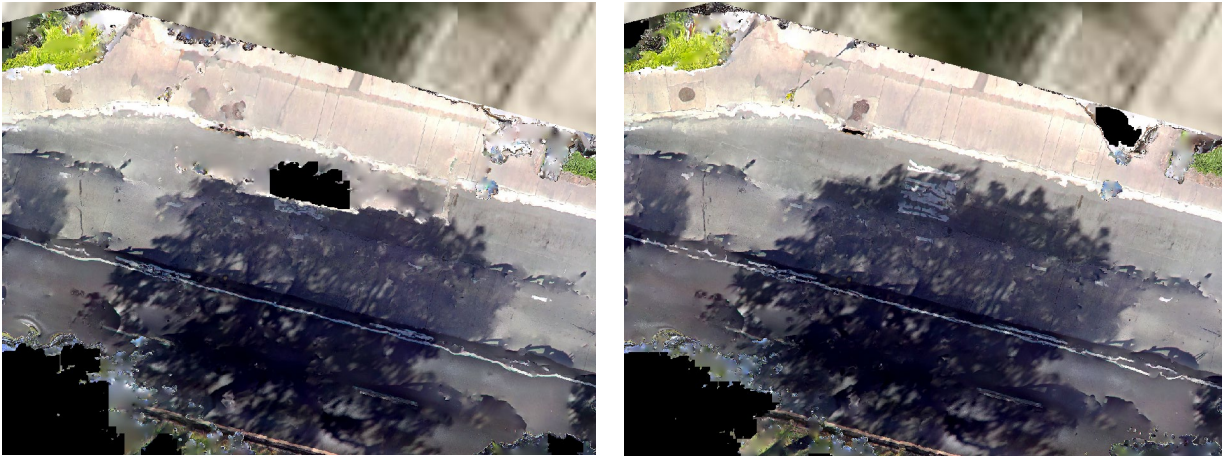


Fig. 19. Masking the cars on the roadway at Kuhio shows substantial improvements on orthomosaic (a: before, b: after) quality.

For Ala Manoa, the masking of driving cars also slightly improved the quality of orthomosaic (Fig. 20).



(a)

(b)

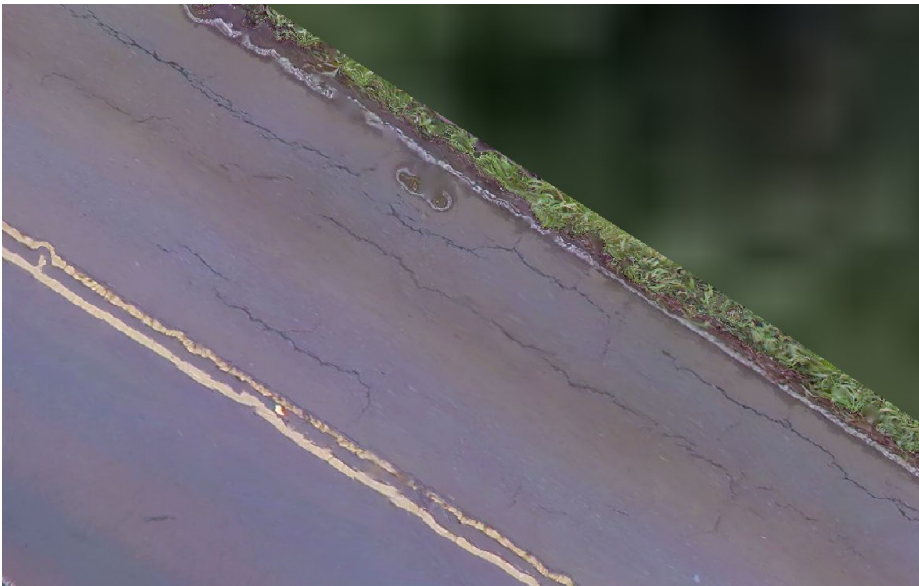
Fig. 20. Masking the cars on the Ala Manoa Boulevard shows slight improvements on orthomosaic (a: before, b: after) quality.

Visual Assessment of Road Conditions and Damage

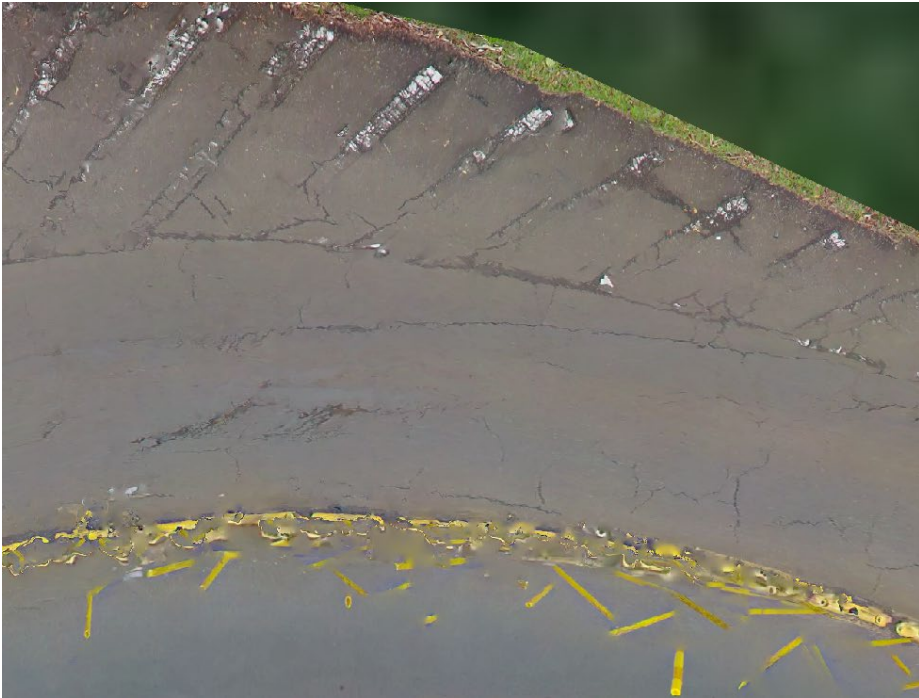
The assessment of road conditions and damage is straightforward on the orthomosaics, which are georeferenced and at an ultra-high spatial resolution (mm level). Fig. 21 shows some examples of the zoom-in snapshots of the road surface, where cracks are clearly visible and can be precisely measured.



(a)



(b)



(c)



(d)



Fig. 21. Examples of georeferenced orthomosaics of roadway.

Conclusions

In this project, we developed a novel methodology of generating georeferenced, very detailed (at millimeter spatial resolution) orthomosaics of road surface using panoramic photos taken from mobile camera system and Structure-from-Motion technology. Our methodology features the importance of masking ego-vehicle (the vehicle that carries the camera), sky, and moving objects (cars, bikes, and pedestrians) on the street captured in the photos. We combined deep learning, image processing, and manual editing approaches to mask these objects. It was found that the masking of these objects from the photos makes it possible to conduct proper photo alignment and, in many cases, can significantly improve the quality of orthomosaics. The final orthomosaics can be easily used for GIS analysis and road condition and damage assessment. In the future, this methodology can be further improved by more automatic masking of these objects, especially with deep learning models. We also found that the timing of capturing the photos can have impacts on the quality of orthomosaic and near noon is a better time window than early morning or later afternoon to minimize the shadows in the orthomosaics.

References

- Chen, L. C., Zhu, Y., Papandreou, G., Schroff, F., & Adam, H. (2018). Encoder-decoder with atrous separable convolution for semantic image segmentation. In *Proceedings of the European conference on computer vision (ECCV)* (pp. 801-818).
- Fletcher, C., Boyd, R., Neal, W. J., & Tice, V. (2010). *Living on the shores of Hawaii: Natural hazards, the environment, and our communities*. University of Hawai'i Press.
- Ghaffarian, S., Kerle, N., & Filatova, T. (2018). Remote sensing-based proxies for urban disaster risk management and resilience: A review. *Remote Sensing*, 10(11), 1760.
- Gong, J., & Maher, A. (2014). Use of mobile lidar data to assess hurricane damage and visualize community vulnerability. *Transportation Research Record*, 2459(1), 119-126.
- Hartley, R., & Zisserman, A. (2003). *Multiple View Geometry in Computer Vision*. Cambridge University Press, Cambridge, UK.
- Hawai'i Climate Change Mitigation and Adaptation Commission (HCCMAC) (2017). *Hawai'i Sea Level Rise Vulnerability and Adaptation Report*. Prepared by Tetra Tech, Inc. and the State of Hawai'i Department of Land and Natural Resources, Office of Conservation and Coastal Lands, under the State of Hawai'i Department of Land and Natural Resources Contract No: 64064.
- Jalinoos, F., Agrawal, A. K., Brooks, C. N., Amjadian, M., Banach, D. M., Boren, E. J., ... & Ahlborn, T. M. (2019). Post-hazard engineering assessment of highway structures using remote sensing technologies (No. FHWA-HIF-20-004). United States. Federal Highway Administration. Office of Infrastructure Research and Development.
- Ji, S., Qin, Z., Shan, J., & Lu, M. (2020). Panoramic SLAM from a multiple fisheye camera rig. *ISPRS Journal of Photogrammetry and Remote Sensing*, 159, 169-183.
- Koks, E. E., Rozenberg, J., Zorn, C., Tariverdi, M., Vousdoukas, M., Fraser, S. A., ... & Hallegatte, S. (2019). A global multi-hazard risk analysis of road and railway infrastructure assets. *Nature Communications*, 10(1), 1-11.
- Martin, M. A., Jahanger, Q. K., Zimmerman, G., Hadziomerspahic, A., Sillars, D. N., Ng, E. H., & Calvo-Amodio, J. (2020). Case study: Economic analysis of statewide roadway 3D mapping using mobile LiDAR. *Journal of Transportation Engineering, Part A: Systems*, 146(7), 05020004.
- Olsen, M. J. (2013). Guidelines for the use of mobile LIDAR in transportation applications (Vol. 748). *Transportation Research Board*.

Onat, Y., Francis, O. P., & Kim, K. (2018). Vulnerability assessment and adaptation to sea level rise in high-wave environments: A case study on O'ahu, Hawai'i. *Ocean & Coastal Management*, 157, 147-159.

Schnebele, E., Tanyu, B. F., Cervone, G., & Waters, N. (2015). Review of remote sensing methodologies for pavement management and assessment. *European Transport Research Review*, 7(2), 1-19.

Seydi, S. T., & Rastiveis, H. (2019). A deep learning framework for roads network damage assessment using post-earthquake lidar data. *International Archives of the Photogrammetry, Remote Sensing & Spatial Information Sciences*, Volume XLII-4/W18, 955-961.

Wang, Y., Chen, Q., Zhu, Q., Liu, L., Li, C., & Zheng, D. (2019). A survey of mobile laser scanning applications and key techniques over urban areas. *Remote Sensing*, 11(13), 1540.

Data Management Plan

Products of Research

The 360-degree panoramic photos were captured using a NCTECH iStar Pulsar mobile mapping system provided by NDPTC. A total of 102, 272, and 100 panoramic photos were used in Kuhio, Ala Manoa, and UH, respectively, for our data analysis. Orthomosaics were generated from these photos using the methodology developed in this study and the Structure-from-Motion technique.

Data Format and Content

Each of the panoramic photos has a size of 11000x5500 pixels and is stored in JPG format. These panoramic photos were derived from photos from four cameras in the mobile mapping system. Each orthomosaic file was stored in GEOTIFF format with the WGS84 geographic coordinate system.

Data Access and Sharing

The panoramic photos and orthomosaics can be accessed from the Dryad website <https://datadryad.org/stash/dataset/doi:10.5061/dryad.4mw6m90jc>.

Reuse and Redistribution

There are no restrictions to reuse or redistribute the data by the general public.